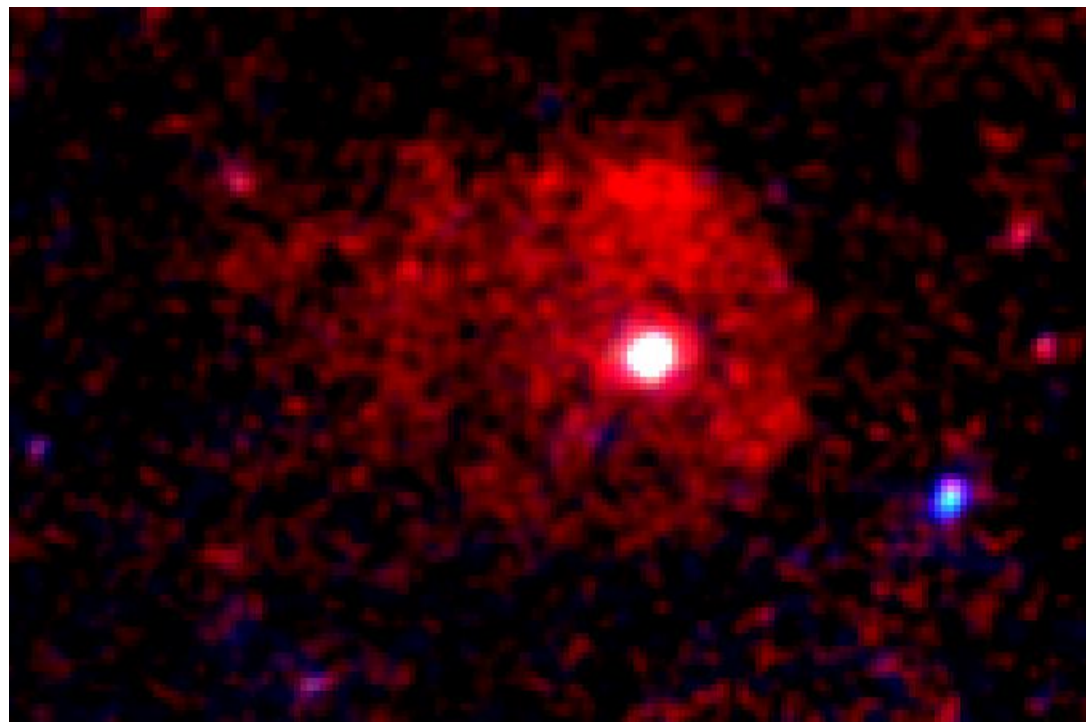


IKT 16: A Composite SNR in the SMC



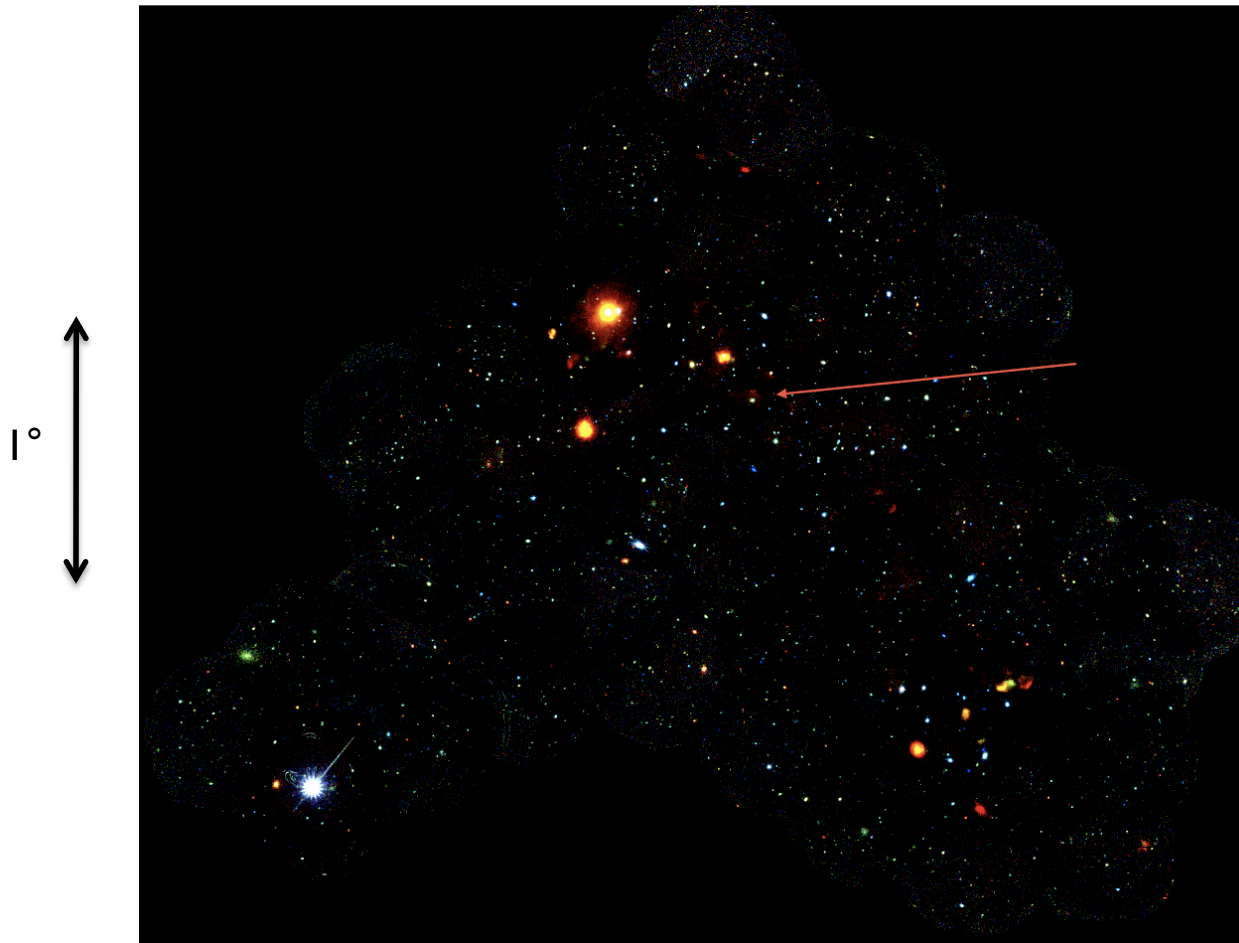
R. Owen, M. Filipovic, J. Ballet
and the SMC XMM-Newton Large Project collaboration

Owen et al. 2011, A&A, 530, 132

SMC XMM-Newton Large Project

30 fields in the SMC observed by XMM-Newton (≈ 30 ks each).

Combined with archive observations, this survey provides complete coverage.



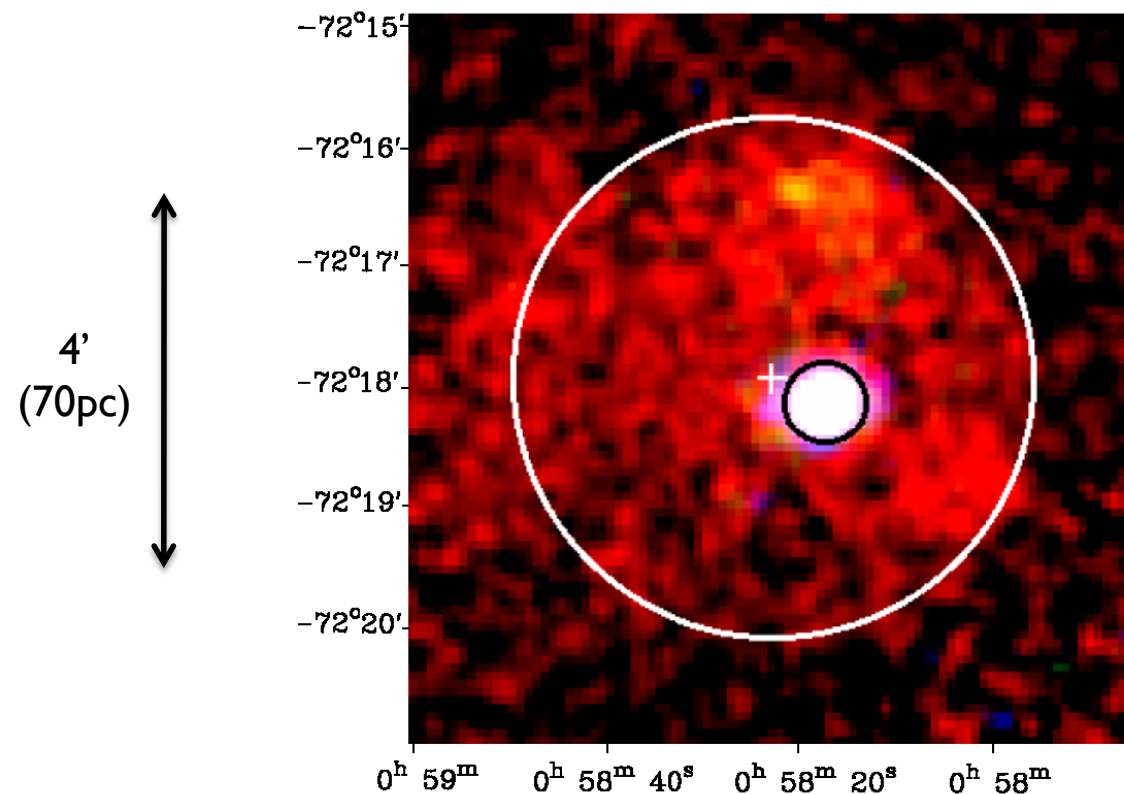
RGB XMM-Newton
mosaic image
(courtesy S. Snowden).
Red: 0.2-1 keV
Green: 1-2 keV
Blue: 2-4.5 keV

IKT 16

X-ray and radio-faint SNR in the SMC bar.

Discovered as candidate SNR with Einstein by Inoue et al. (1983).

Properties first studied using XMM-Newton by van der Heyden et al. (2004).



XMM-Newton mosaic
RGB image of IKT 16.
Red: 0.3-0.8 keV
Green: 0.8-1.2 keV
Blue: 1.2-2 keV

IKT 16

X-ray and radio-faint SNR in the SMC bar.

Discovered as candidate SNR with Einstein by Inoue et al. (1983).

Properties first studied using XMM-Newton by van der Heyden et al. (2004).

Observation ID	Start Date (yyyy-mm-dd)	Filter ^a pn/MOS1/MOS2	Pointing co-ordinates		Useful exposure (ks)		
			RA (J2000)	Dec (J2000)	pn	MOS 1	MOS2
0018540101	2001-11-20	M/M/M	00 ^h 59 ^m 26.8 ^s	-72° 09' 55''	23.4 ^b	18.1 ^b	18.0 ^b
0084200101	2002-03-30	T/M/M	00 ^h 56 ^m 41.7 ^s	-72° 20' 11''	8.8	10.0	10.3
0110000201	2000-10-17	M/M/M	00 ^h 59 ^m 26.0 ^s	-72° 10' 11''	14.3 ^b	16.7 ^b	16.8 ^b
0212282601	2005-03-27	-/M/M	00 ^h 59 ^m 26.8 ^s	-72° 09' 54''	0.0	3.8	3.8
0304250401	2005-11-27	M/M/M	00 ^h 59 ^m 26.8 ^s	-72° 09' 54''	15.9	17.4 ^b	17.4 ^b
0304250501	2005-11-29	M/M/M	00 ^h 59 ^m 26.8 ^s	-72° 09' 54''	14.9	16.5 ^b	16.6 ^b
0304250601	2005-12-11	M/M/M	00 ^h 59 ^m 26.8 ^s	-72° 09' 54''	10.6	16.4 ^b	16.2 ^b
0500980201	2007-06-06	T/M/M	01 ^h 00 ^m 00.0 ^s	-72° 27' 00''	14.8	23.2	23.9 ^b
0601210801	2009-10-09	T/M/M	00 ^h 56 ^m 15.5 ^s	-72° 21' 55''	23.0 ^b	24.6	24.6 ^b

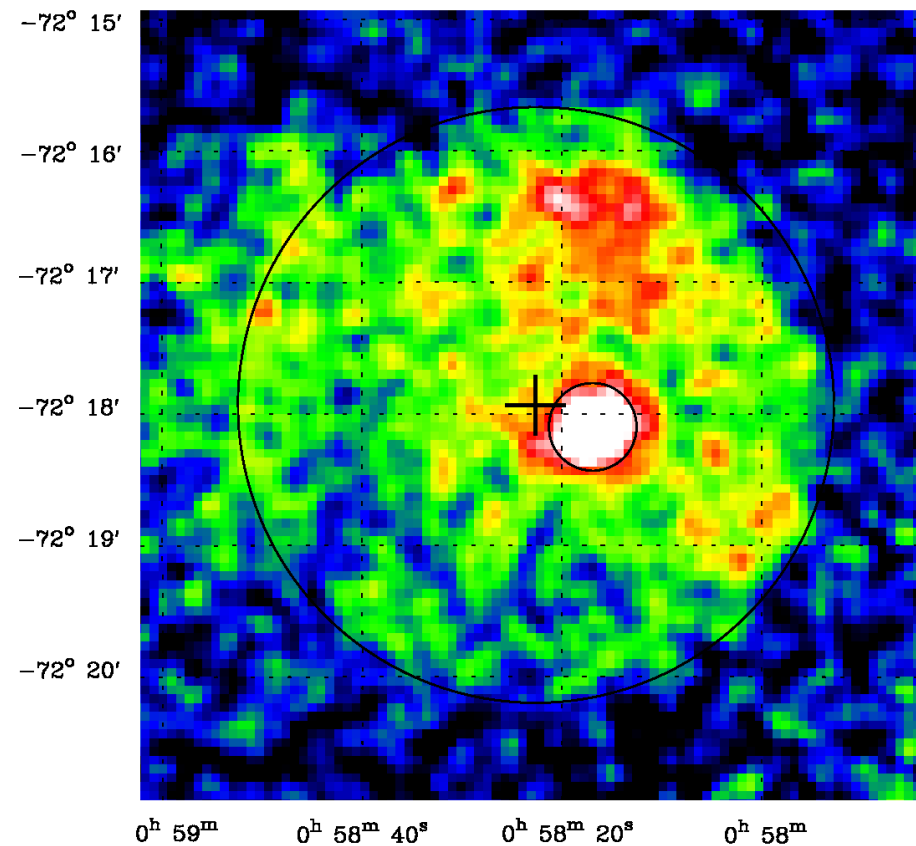
^a - T = thin filter, M = Medium filter.

^b - Observation used for spectral analysis.

Mosaic X-ray image

X-ray radius of IKT 16 = 128'' (37 pc at a distance of 60 kpc).

Distance between SNR centre and point source $\approx 30''$.

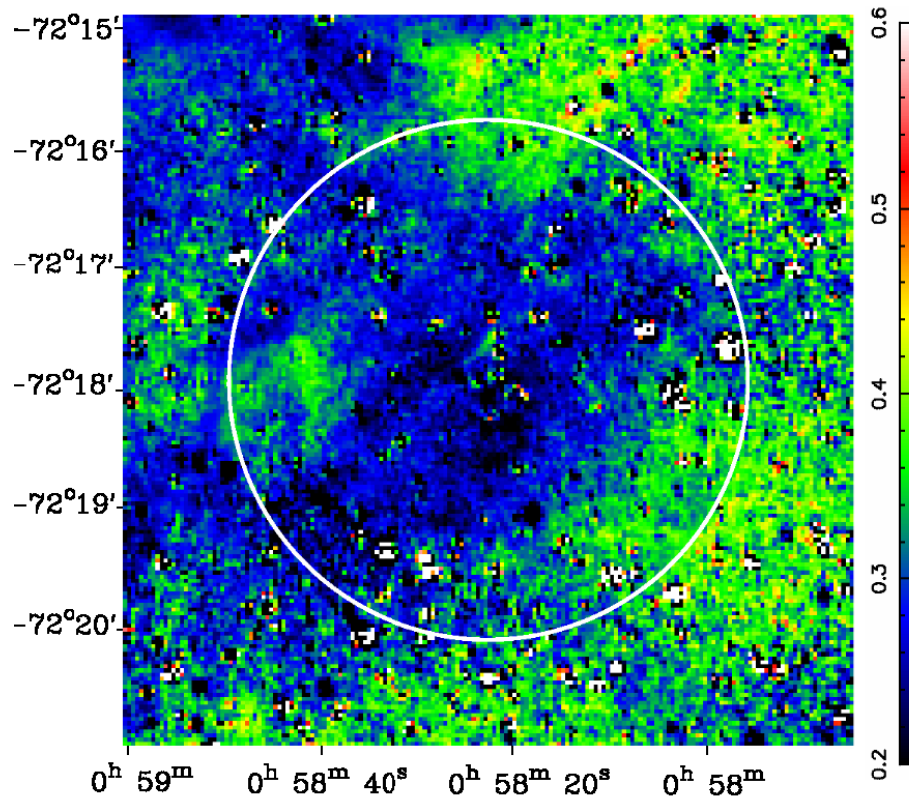


XMM-Newton mosaic soft X-ray (0.3-1 keV) image of IKT 16.

Multiwavelength observations

Radio data: ATCA ($\lambda = 3\text{cm}, 6\text{cm}, 13\text{cm}, 20\text{cm}$) and MOST ($\lambda = 36\text{cm}$).

Optical data: MCELS survey ($\text{H}\alpha$, SII , OIII emission lines).

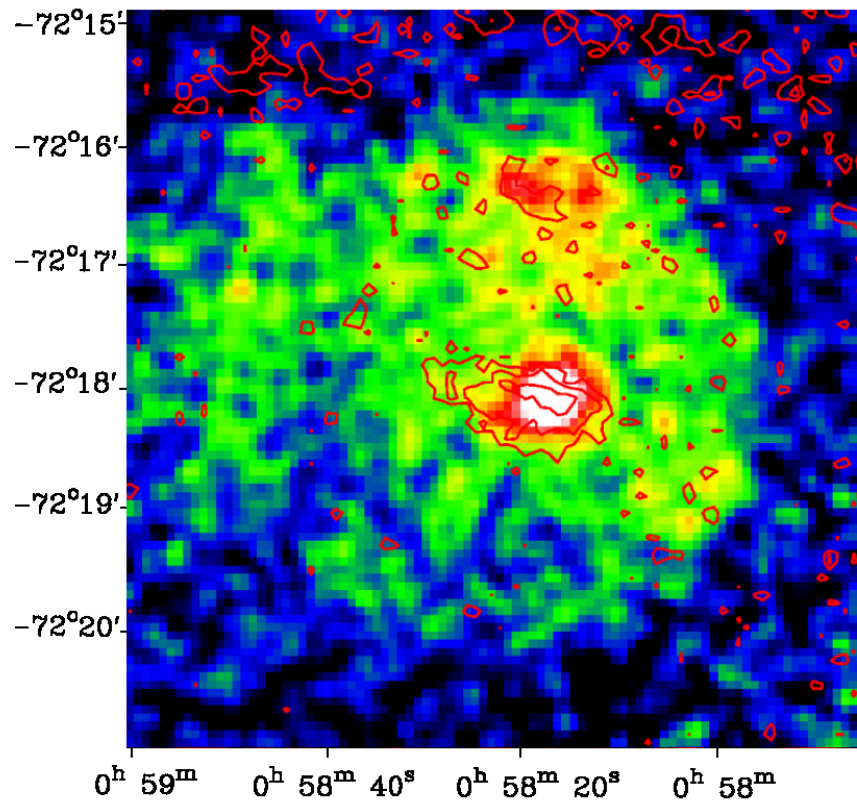


$\text{SII}/\text{H}\alpha$ ratio across IKT 16.
Typical values for radiative shocks in SMC SNRs > 0.4 .

Multiwavelength observations

Radio data: ATCA ($\lambda = 3\text{cm}, 6\text{cm}, 13\text{cm}, 20\text{cm}$) and MOST ($\lambda = 36\text{cm}$).

Optical data: MCELS survey ($\text{H}\alpha$, SII , OIII emission lines).

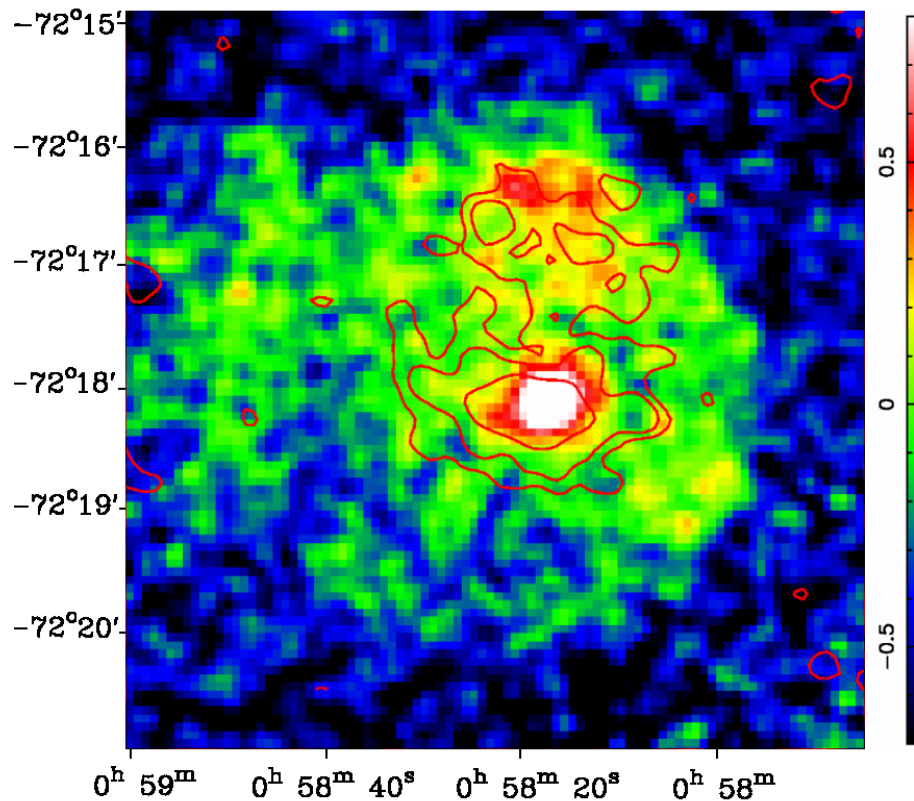


20cm ATCA radio contours
on soft X-ray image.

Multiwavelength observations

Radio data: ATCA ($\lambda = 3\text{cm}, 6\text{cm}, 13\text{cm}, 20\text{cm}$) and MOST ($\lambda = 36\text{cm}$).

Optical data: MCELS survey ($\text{H}\alpha, \text{SII}, \text{OIII}$ emission lines).

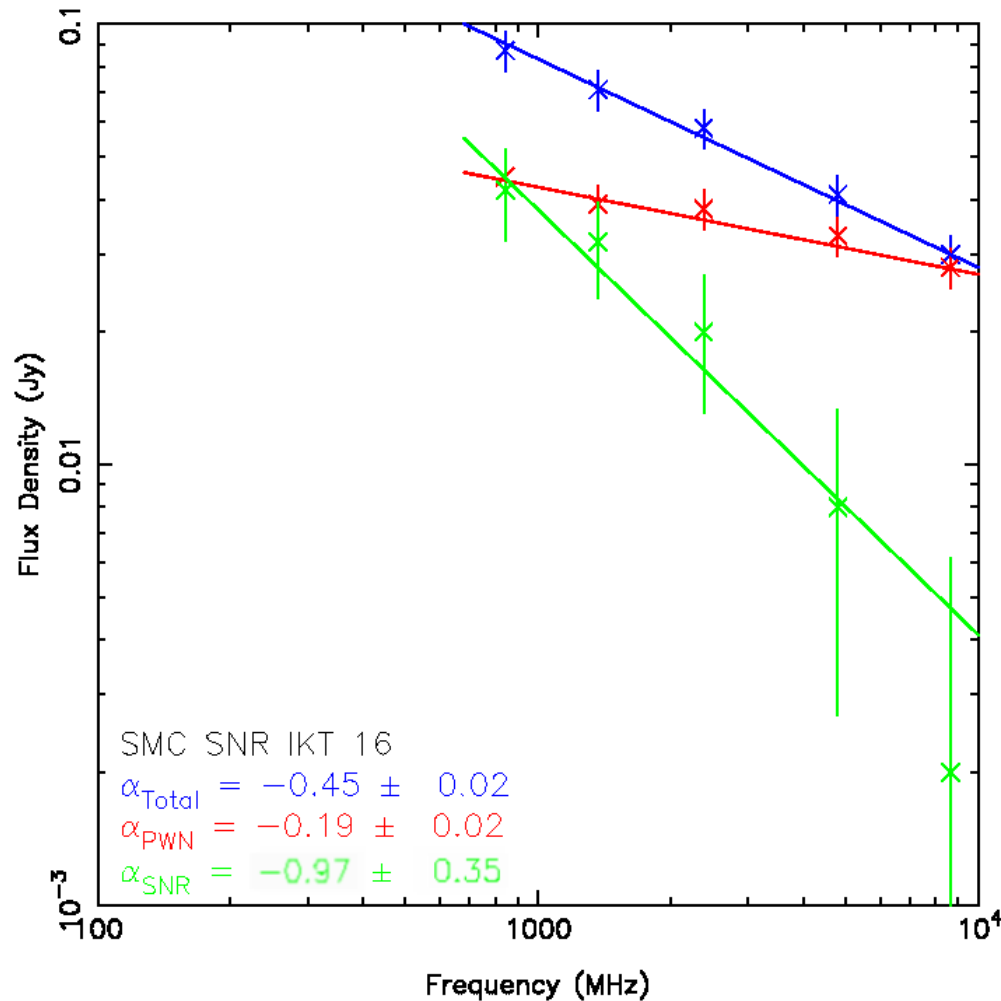


3cm ATCA radio contours on soft X-ray image.

Multiwavelength observations

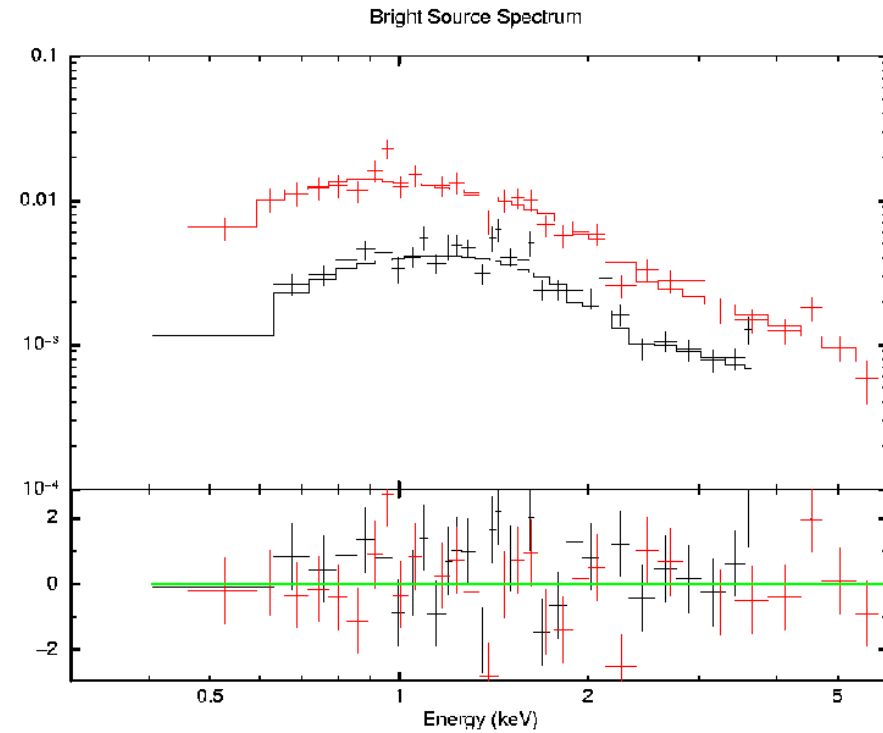
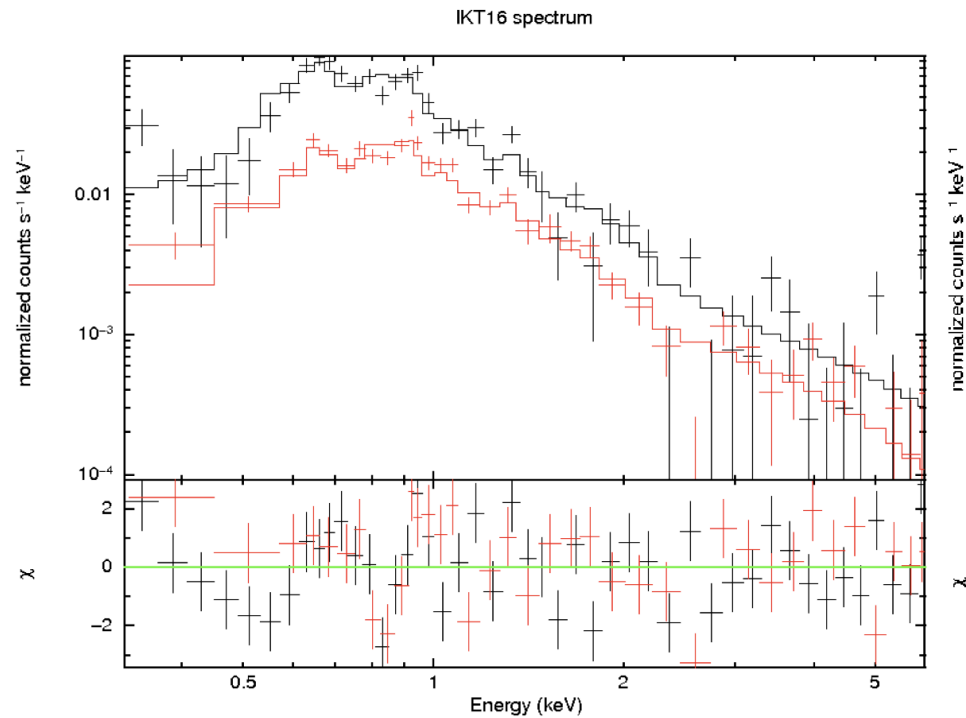
Radio data: ATCA ($\lambda = 3\text{cm}, 6\text{cm}, 13\text{cm}, 20\text{cm}$) and MOST ($\lambda = 36\text{cm}$).

Optical data: MCELS survey ($\text{H}\alpha, \text{SII}, \text{OIII}$ emission lines).



Radio spectra of the entire system (blue), central source (red) and the SNR (green).

X-ray spectral analysis



X-ray spectral analysis

Table 3. Parameters of the best-fit model to SNR and bright source regions.

Region	SMC Absorption 10^{21}cm^{-2}	Power-law Cont. Photon Index Normalization	Sedov model		Goodness of Fit χ^2/dof	Unabsorbed L_X^a 0.5–10 keV (10^{35}erg s^{-1})
			Shock T (keV) Normalization	Ion. time ($10^{10}\text{cm}^{-3}\text{s}$)		
SNR	3.4(f)	1.58(f) $1.0 \times 10^{-5}(\text{f})$	1.03 ± 0.12 $1.4 \pm 0.3 \times 10^{-4}$	6.1	1103/1032	1.6 ± 0.4
Bright Source	3.4 ± 0.6	1.58 ± 0.07 $3.4 \pm 0.4 \times 10^{-5}$	$1.03(\text{f})$ $3.6 \times 10^{-6}(\text{f})$	$6.1(\text{f})$	150/137	1.6 ± 0.2

^a - Includes correction for spillover of bright source photons into SNR extraction area and vice versa.
(f) - Parameter fixed for consistency between fit regions.

Absorption column in SMC in this direction = $5.7 \times 10^{21}\text{cm}^{-2}$.

Sedov-phase SNR properties

$$n_e = \sqrt{\frac{3D^2N}{10^{-24}R^3}}, \text{ m}^{-3}$$

$$t_{dyn} = \frac{1.3 \times 10^{-14}R}{\sqrt{T_s}}, \text{ yr}$$

$$M = 5 \times 10^{-31}m_p r_m n_e V, \text{ M}_\odot$$

$$E_0 = 2.64 \times 10^{-8}T_s R^3 n_e, \text{ erg}$$

$$I_t = 4 \times 10^{-6}n_e t_{dyn}, \text{ m}^{-3}\text{s}$$

Studying the morphology of the remnant gives radius R , volume V (at distance D)

From spectral analysis, we find shock temperature T_s and normalization N .

From these, we can derive:

- Electron density (n_e)
- Dynamical age (t_{dyn})
- Mass swept-up by SNR (M)
- Initial Explosion energy (E_0)

Properties of the SNR

Parameter	Units	This paper	VDH04
Temperature	keV	1.03	1.76
Radius	pc	37	29
Electron Density	cm^{-3}	0.03	0.05/0.04 ^a
Dynamical age	yr	14700	7500
Swept-up mass	M_{\odot}	232	124
Explosion energy	10^{51} erg	1.2	3.4

^a - VDH04 derive electron and proton densities separately, assumed to be approximately the same here.

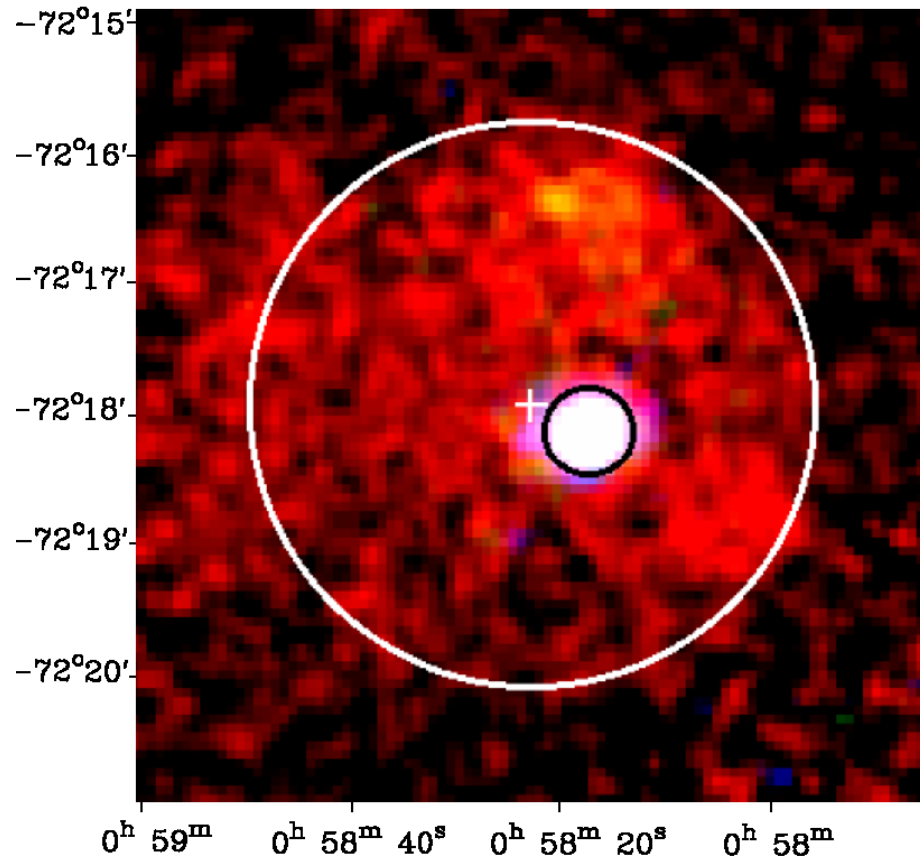
Our derived SNR properties differ significantly from van der Heyden et al (2004).

Temperature is lower (closer to typical X-ray temperature for gas in SNR).

Age consistent with Sedov phase remnant.

Low density environment.

What is the nature of the bright source?



Several possible source types:

Foreground source / Background AGN

Pulsar Wind Nebula (PWN)

Microquasar

Foreground Galactic source / AGN?

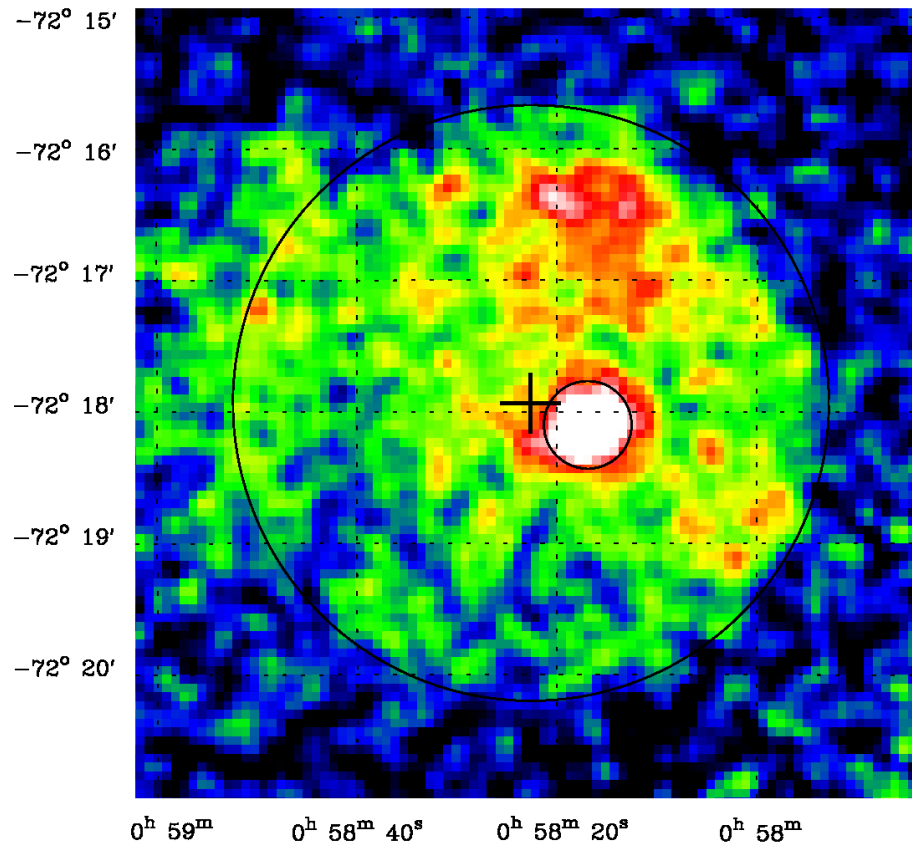
Foreground source:

- PL spectrum more absorbed than Galactic N_{H} ($\approx 3 \times 10^{21}$ cf. $6 \times 10^{20} \text{ cm}^{-2}$).
- Absorption consistent with that at position of SNR.
- Difficult to fit with simple models / explain extended radio emission.

AGN:

- Index of PL fit ($\Gamma=1.6$) consistent with Type I AGN.
- Reasonable soft excess required to balance necessary extra absorption.
- No optical counterpart in OGLE survey (to $V=21.5$) to 2σ position error.
- We expect to see one (at $V \approx 15-20$) for a source with this X-ray flux.
- Statistical probability of AGN at this flux within $30''$ of SNR centre – 0.07%.

Dynamics of the source



X-ray point source $30 \pm 8''$ from centre.

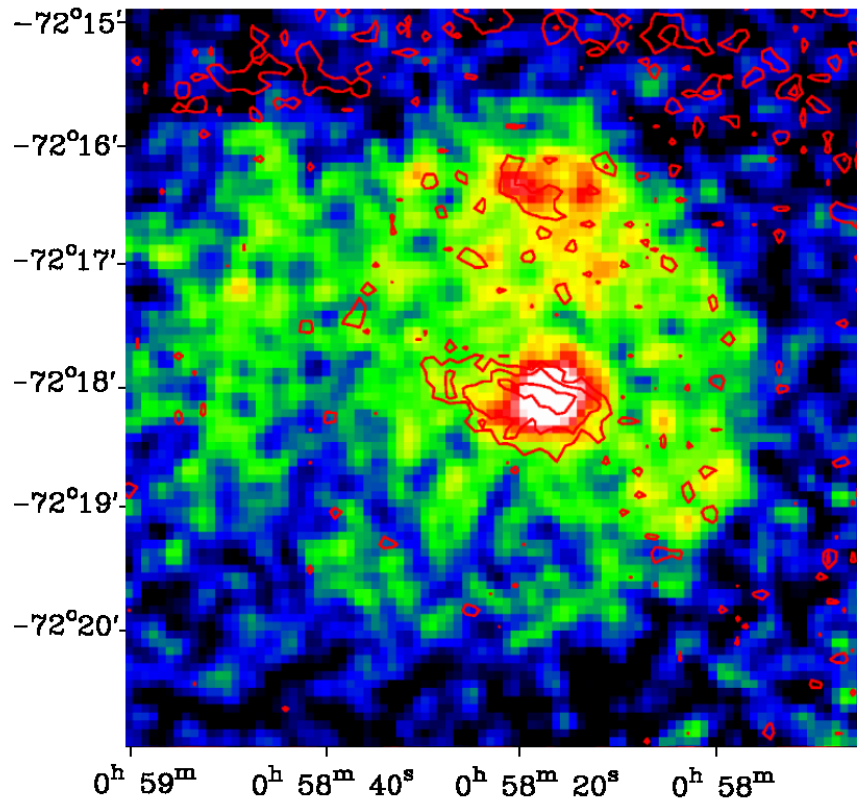
In plane of SNR (at 60kpc), this is 8 ± 2 pc.

SNR age ≈ 14500 yr

Kick velocity ≈ 580 ($/\cos i$) ± 100 km s⁻¹.

Typical compact object velocity ≈ 500 km s⁻¹.
(Lyne & Lorimer 1994)

Pulsar Wind Nebula?



20cm radio contours on soft X-ray image.

Generated by dissipation of pulsar's rotational energy through relativistic winds (Gaensler & Slane 2006).

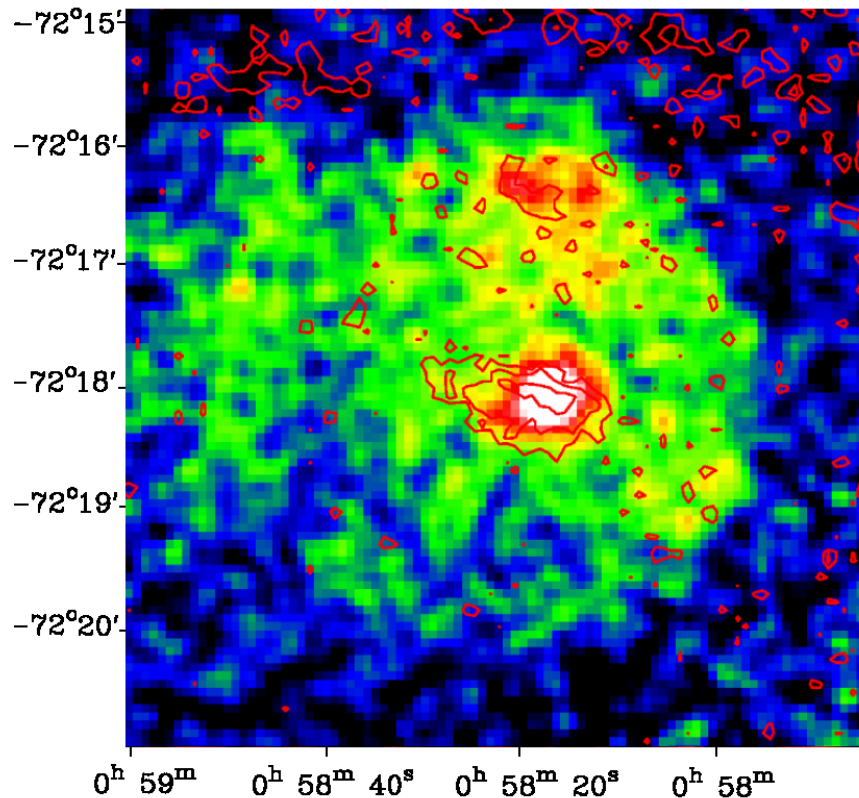
X-ray spectrum: PL index $1.1 < \Gamma < 2.3$.

Radio emission more extended due to longer cooling time, may trace path of source.

Radio emission of PWNe shows flat spectral index ($-0.3 < \alpha$). $\alpha = -0.2$ here.

However – point source in XMM-Newton, PWNe are usually seen as extended sources.

Microquasar?



20cm radio contours on soft X-ray image.

X-ray emission from XRB, radio emission seen from relativistic jets.

X-ray spectrum: PL index $1.5 < \Gamma < 2.2$.

Radio jets observed with steep spectral index ($-0.8 < \alpha < -0.4$).

Typical LMXB kick velocity: $180 \pm 80 \text{ km s}^{-1}$
(cf. inferred velocity of $> 450 \text{ km s}^{-1}$).
Typical HMXB velocity lower still.

Orientation of radio jet should be random, coincidental pointing towards SNR centre?

No evidence of X-ray variability!

Conclusions

IKT 16 is a SNR in the Sedov-adiabatic phase of evolution.

Low n_e , large size, high T and moderate N_H suggest it is in low density environment near the centre of the SMC.

X-ray point source observed is likely associated with the SNR.

PWN or microquasar origins are examined, with PWN much more likely. Chandra observation will determine extent of X-ray source.

If confirmed as PWN, this is the first known composite SNR in the SMC.